Therapy-induced malignant neoplasms in *Nf1* mutant mice

Richard C. Chao,[1,8,11] Urszula Pyzel,[1] Jane Fridlyand,[2] Yien-Ming Kuo,[1,3] Lewis Teel,[1] Jennifer Haaga,[1] Alexander Borowsky,[9] Andrew Horvai,[4] Scott C. Kogan,[5,6] Jeannette Bonifas,[1] Bing Huey,[6] Tyler E. Jacks,[10] Donna G. Albertson,[5,6,7] and Kevin M. Shannon[1,6,*]

[1]Department of Pediatrics, University of California, San Francisco, San Francisco, California 94143
[2]Department of Epidemiology and Biostatistics, University of California, San Francisco, San Francisco, California 94143
[3]Department of Medicine, University of California, San Francisco, San Francisco, California 94143
[4]Department of Pathology, University of California, San Francisco, San Francisco, California 94143
[5]Department of Laboratory Medicine, University of California, San Francisco, San Francisco, California 94143
[6]Comprehensive Cancer Center, University of California, San Francisco, San Francisco, California 94143
[7]Cancer Research Institute, University of California, San Francisco, San Francisco, California 94143
[8]Department of Medicine, Division of Hematology/Oncology, Department of Veterans' Affairs Medical Center, San Francisco, California 94121
[9]Medical Pathology Center for Comparative Medicine, University of California, Davis, Davis, California 95616
[10]Center for Cancer Research, Massachusetts Institute of Technology, Cambridge, Massachusetts 02139
[11]Present address: Pfizer Global Research and Development, 10578 Science Center Drive (B95), San Diego, California 92121
*Correspondence: kevins@itsa.ucsf.edu

Summary

Therapy-induced cancers are a severe complication of genotoxic therapies. We used heterozygous *Nf1* mutant mice as a sensitized genetic background to investigate tumor induction by radiation (RAD) and cyclophosphamide (CY). Mutagen-exposed *Nf1*$^{+/-}$ mice developed secondary cancers that are common in humans, including myeloid malignancies, sarcomas, and breast cancers. RAD cooperated strongly with heterozygous *Nf1* inactivation in tumorigenesis. Most of the solid tumors showed loss of the wild-type *Nf1* allele but retained two *Trp53* alleles. Comparative genomic hybridization demonstrated distinct patterns of copy number aberrations in sarcomas and breast cancers from *Nf1* mutant mice, and tumor cell lines showed deregulated Ras signaling. *Nf1*$^{+/-}$ mice provide a tractable model for investigating the pathogenesis of common mutagen-induced cancers and for testing preventive strategies.

Introduction

Therapy-induced malignant neoplasms, also known as second malignant neoplasms (SMNs), are a severe complication of genotoxic cancer treatments including radiation (RAD) and chemotherapeutic agents (Bhatia and Sklar, 2002; Matesich and Shapiro, 2003; Smith et al., 2003). SMNs have a substantial public health impact, as they account for most of the ~90,000 new cancers that are diagnosed in the United States each year in persons who had a previous histologically distinct malignancy (Bhatia and Sklar, 2002). Whereas early reports emphasized the risk of SMNs in patients with Hodgkin's disease and other hematopoietic malignancies (Le Beau et al., 1986; Rowley et al., 1977; Tucker et al., 1988), these cancers are increasingly recognized after intensive treatment for breast cancer and other solid tumors (Matesich and Shapiro, 2003; Smith et al., 2003). Myeloid leukemia, lymphoma, and sarcoma are the most common SMNs found in survivors of hematologic and nonhematologic cancers (Bhatia and Sklar, 2002; Matesich and Shapiro, 2003; Smith et al., 2003). With prolonged follow-up, cancer survivors are also at elevated risk of developing epithelial tumors of the breast, uterus, and gastrointestinal tract (de Vathaire et al., 1989a, 1989b; Hawkins et al., 1987; Tucker et al., 1988). Importantly, many SMNs are resistant to treatment, and previous exposure to cytotoxic agents may limit the use of intensive salvage regimens. The lack of relevant animal models of SMNs has impeded efforts to understand how mutagenic cancer therapeutics induce tumors in vivo, and to test preventive strategies.

Studies of familial cancer syndromes have provided fundamental insights into mechanisms that underlie tumorigenesis. In addition to markedly increasing the incidence of primary ma-

SIGNIFICANCE

Cancers induced by genotoxic treatments are a major clinical problem; however, the long-term mutagenic potential of specific therapeutic regimens may not be known until many years from now. We used *Nf1* mutant mice to recapitulate the dynamic interaction between mutagen exposure and tumorigenesis that underlies the development of human therapy-induced malignancies. These animals develop a similar spectrum of malignancies as human patients who are treated with radiation and alkylating agents, and provide a tractable system for performing mechanistic studies, for comparing the mutagenic potential of different regimens, and for testing preventive strategies. Our data also have translational implications for assessing the potential risks of genotoxic modalities, particularly in persons with neurofibromatosis type 1.

lignancies, some inherited cancer predispositions confer a high risk of SMNs. For example, persons with the Li-Fraumeni syndrome carry germline *TP53* mutations, which leads to an elevated risk of both primary malignancies and SMNs (Li and Fraumeni, 1982; Malkin et al., 1992; Nichols et al., 2001). Similarly, most children with a germline *RB1* mutation develop one or more retinoblastoma tumors and are predisposed to osteosarcoma and other cancers later in life (Wong et al., 1997). The incidence of osteosarcoma is dramatically increased in areas exposed to RAD in the course of treating the initial retinoblastoma (Wong et al., 1997). As in de novo cancers, investigating how heritable mutations cooperate with genotoxic cancer therapies will likely provide mechanistic insights that are relevant to tumorigenesis in individuals who develop SMNs without a known genetic predisposition.

Mutations in the *NF1* tumor suppressor gene cause neurofibromatosis type 1 (NF1), an inherited cancer syndrome that affects 1 in 3500 persons (Cichowski and Jacks, 2001; Dasgupta and Gutmann, 2003). *NF1* encodes neurofibromin, a GTPase-activating protein that negatively regulates Ras signaling (Boguski and McCormick, 1993; Donovan et al., 2002b). Affected individuals are predisposed to specific benign and malignant tumors, particularly in tissues derived from the embryonic neural crest (Side and Shannon, 1998). In addition, the incidence of juvenile myelomonocytic leukemia (JMML) and other myeloid malignancies is increased 200- to 500-fold in children with NF1 (Stiller et al., 1994). Clinical data suggest that persons with NF1 are also predisposed to SMNs. Maris and coworkers (Maris et al., 1997) reported five children with NF1 who developed myeloid malignancies and performed a systematic review of 64 children with NF1 who received chemotherapy and/or RAD to treat a primary cancer. This study revealed an 11% incidence of SMNs, with an especially high risk in children who had a primary embryonal cancer. Two adults with NF1 also developed therapy-related myelodysplastic syndrome (MDS) after treatment for de novo acute myeloid leukemia (AML) (Papageorgio et al., 1999). These reports suggested that therapeutic exposure to genotoxic agents might cooperate with germline *NF1* mutations in the genesis of common SMNs found in the general population, namely myeloid leukemia and sarcoma.

Based on these clinical observations, we reasoned that heterozygous *Nf1* mutant mice (*Nf1*$^{+/-}$) might be harnessed to investigate the pathogenesis of SMNs in vivo. *Nf1*$^{+/-}$ mice spontaneously develop pheochromocytoma and a myeloproliferative disorder (MPD) that resembles JMML with incomplete penetrance (Jacks et al., 1994b). In a previous study, exposing these mice to the alkylating agent cyclophosphamide (CY) increased the incidence of MPD and reduced the latency (Mahgoub et al., 1999). Here, we show that RAD alone or in combination with CY induces a spectrum of SMNs in *Nf1*$^{+/-}$ mice that includes soft tissue sarcomas and breast carcinomas. The normal *Nf1* allele is inactivated in most of these solid tumors, and some also demonstrate loss of heterozygosity (LOH) at the *Trp53* locus. Comparative genomic hybridization (CGH) uncovered tumor-specific patterns of copy number aberrations, which implies the existence of distinct pathways of cooperating genetic lesions in different cancers. Biochemical investigation of cell lines developed from a subset of these malignant tumors revealed deregulated Ras signaling. *Nf1*$^{+/-}$ mice provide a tractable in vivo model for understanding how RAD and alkylating agents induce cancer, and for testing preventive strategies.

Results

CY and RAD induce reversible myelosuppression

We selected CY for investigation because this alkylating agent is a component of many front-line therapeutic regimens. To model the myelosuppression that occurs in human patients, we intercrossed wild-type C57Bl/6 and 129/Sv mice to generate cohorts of five to ten F1 animals that were exposed to different CY doses. Mice injected with a weekly intraperitoneal CY dose of 200 mg/kg for 6 consecutive weeks reproducibly developed anemia and leukopenia that resolved after the drug was discontinued (data not shown). This regimen was not otherwise associated with obvious morbidity. A single RAD dose of 3 Gy, which was selected on the basis of previous data showing that this dose was leukemogenic in CBA mice (Major, 1979; Major and Mole, 1978; Mole et al., 1983), was administered 2 weeks after the last dose of CY. In a pilot experiment that assessed the combination of CY at 200 mg/kg/week for 6 weeks followed by 3 Gy of RAD, we found that mice tolerated sequential treatment without significant toxicity (data not shown).

Based on these preliminary data, 192 wild-type and *Nf1*$^{+/-}$ mice were assigned to one of four groups at 8–17 weeks of age: no treatment, CY only, RAD only, or CY followed by RAD. Treatment with CY, RAD, or the combination resulted in reversible myelosuppression (Figure S1 in the Supplemental Data available with this article online). Mice that received six weekly injections of CY developed anemia with decreases in hemoglobin concentration (from 16.2 ± 1.0 g/dl to 12.3 ± 1.3 g/dl; $p < 0.00001$) and white blood cell count (from $7.4 \pm 3.0 \times 10^3$ to $1.5 \pm 0.7 \times 10^3$ cells/μl; $p < 0.00001$). Animals assigned to receive RAD alone entered the study cohort concurrently and were irradiated at the same time as mice that had been treated with CY. RAD induced a significant reduction in leukocyte counts and a modest fall in the hemoglobin concentration that was not statistically significant (Figure S1). Myelosuppression was similar in wild-type and *Nf1*$^{+/-}$ mice, and peripheral blood cell counts recovered quickly after cessation of CY and/or RAD. The only early treatment-related deaths occurred 19 and 20 days after RAD in two wild-type mice that received both CY and RAD (~1% of the cohort).

Survival and tumorigenesis in wild-type and *Nf1*$^{+/-}$ mice

Pathologic analysis was performed on 91% of the study cohort, including 97 of 104 wild-type mice and 77 of 86 *Nf1*$^{+/-}$ mice. Three wild-type and four *Nf1*$^{+/-}$ mice were considered evaluable without complete pathologic analysis, including two mice with treatment-related mortality, two mice with massive splenomegaly in which there was no histologic analysis of other organs, and three mice with tumors of the Harderian gland, which secretes lipid and porphyrins over the eye. Eleven mice that died unexpectedly could not be analyzed for tumor formation. Heterozygous inactivation of *Nf1* was strongly associated with an increased risk of premature death following treatment with a survival rate of only 30% after 15 months in *Nf1*$^{+/-}$ mice compared with 78% in wild-type littermates (Figure 1, left panel; $p < 0.001$). Death was due to cancer in 96% of evaluable mice. We identified 51 malignancies in 81 *Nf1*$^{+/-}$ ani-

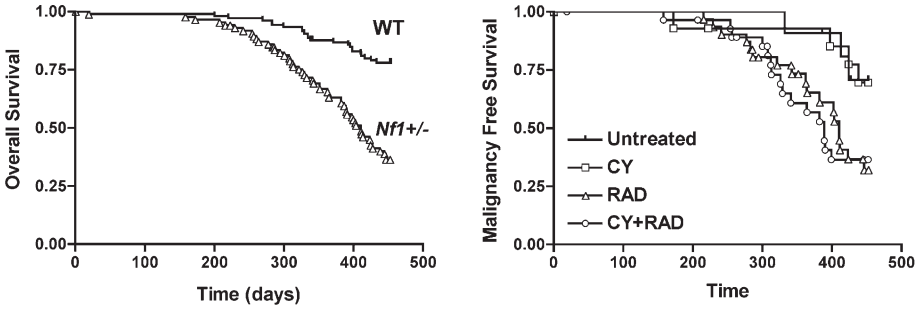

Figure 1. Reduced survival and increased incidence of cancer in *Nf1*$^{+/-}$ mice

Kaplan-Meier analysis was performed to analyze survival and tumor formation in the entire cohort from the date that mice assigned to receive radiation were treated. Left panel: analysis of overall survival demonstrates an increased risk of death in *Nf1*$^{+/-}$ versus wild-type (WT) mice with a hazard ratio of death of 3.83 (confidence interval: 2.52–6.40). The survival plots include control (untreated) and genotoxin-exposed mice of each genotype. Right panel: *Nf1*$^{+/-}$ mice that were exposed to RAD alone (p = 0.0043) or RAD in combination with CY displayed a significantly higher risk of cancer than *Nf1*$^{+/-}$ mice that were not irradiated. The incidence of cancer was not significantly different in control and CY-treated *Nf1*$^{+/-}$ mice. In these plots, the latency to death or tumor was measured from the date of radiation treatment.

mals that were available for pathologic examination compared with 17 cancers in 100 wild-type mice (Table 1; $p < 0.0001$). Tumor types that occurred significantly more often in *Nf1*$^{+/-}$ mice included soft tissue sarcomas ($p = 0.001$), myeloid malignancies ($p = 0.0005$), and pheochromocytomas ($p = 0.0007$). Myeloid malignancies and sarcomas, which are the most common SMNs in human patients, accounted for 24 of the 52 cancers found in *Nf1*$^{+/-}$ mice. We also unexpectedly detected breast cancers in four female *Nf1*$^{+/-}$ mice but observed none in the wild-type animals ($p = 0.04$, Fisher's exact test).

RAD cooperated strongly with heterozygous *Nf1* inactivation in tumorigenesis whether administered alone or after CY (Figure 1, right panel; $p = 0.002$). By contrast, the incidence of cancer was similar in untreated *Nf1*$^{+/-}$ mice and in animals that received CY only (Figure 1, right panel). Interestingly, the nature of the mutagen exposure influenced the tumor spectrum in *Nf1*$^{+/-}$ mice. In particular, RAD alone resulted in a greater frequency of myeloid malignancies, whereas exposure to RAD in combination with CY resulted in a high incidence of solid tumors, including breast cancer (Table 2).

Tumor phenotypes

Sixteen *Nf1*$^{+/-}$ mice developed tumors of presumed neural crest origin, which included soft tissue sarcomas, pheochromocytoma, neuroblastoma, and paraganglioma (Table 1). Pheochromocytomas occurred in both untreated *Nf1*$^{+/-}$ mice and in animals that were exposed to genotoxins, whereas sarcomas, neuroblastomas, and paragangliomas only developed after exposure to CY and/or RAD. None of these tumors occurred in wild-type animals ($p = 0.000001$). Soft tissue sarcomas from *Nf1*$^{+/-}$ mice demonstrated a spindle cell pattern, and some were positive by S100 staining (Figures 2A–2F), which is typical of the malignant peripheral nerve sheath tumors (MPNSTs) that occur in NF1 patients (Weiss et al., 1983; Wick et al., 1987). Most of these tumors arose in close proximity to peripheral nerves, were deep-seated, and ranged from morphologically low-grade spindle cell proliferations with $\leq$1 mitotic figure (mf) per 10 high-power fields (hpf) and minimal nuclear atypia to highly malignant tumors with >50 mf per 10 hpf and highly atypical nuclei. The low-grade tumors were uniformly S100-positive, whereas higher-grade lesions were S100-negative, which is consistent with the pattern of S100 expression in human MPNSTs. Interestingly, areas that were architecturally and cytologically reminiscent of benign Schwann cell proliferations were found immediately adjacent to some of the high-grade sarcomas. We also assessed these tumors for epidermal growth factor receptor (EGFR), p16, and p21 expression. Interestingly, none expressed detectable surface EGFR or nuclear p16, whereas seven of eight were positive for nuclear p21 (Figure 3).

Consistent with previous reports (Jacks et al., 1994b; Mahgoub et al., 1999), *Nf1*$^{+/-}$ mice were predisposed to myeloid malignancies ($p = 0.0065$ versus wild-type littermates). Although the overall incidence of these cancers did not differ in *Nf1*$^{+/-}$ mice according to treatment group, exposure to RAD was associated with an unexpectedly diverse spectrum of myeloid diseases, which included cases that were classified as AML, MDS, or cytopenias without definitive criteria for AML or MDS (Kogan et al., 2002). In addition, two *Nf1*$^{+/-}$ mice that died suddenly without a confirmed cause of death had massive splenomegaly, which suggests an underlying myeloid malignancy (Table 1). All of the wild-type mice with myeloid malignancies were from the RAD treatment group. Interestingly, sequential administration of CY and RAD was associated with fewer myeloid malignancies in heterozygous *Nf1* mutant mice than exposure to either modality alone (Table 1).

Four of twenty-one female *Nf1*$^{+/-}$ mice that received CY + RAD were diagnosed with breast cancers. These tumors were characterized by cytokeratin (Figures 2G–2I), which is consis-

Table 1. Tumor spectra in untreated and genotoxin-exposed mice according to genotype

Type of neoplasm	Wild-type (n = 100)	*Nf1*$^{+/-}$ (n = 81)
Neural crest tumors	0	16
Soft tissue sarcomas	0	8
Pheochromocytoma	0	6
Neuroblastoma/paraganglioma	0	2
Myeloid malignancies*	4	17*
Breast cancer	0	4
Poorly differentiated malignant tumors	0	3
Other	13	11
Total	17	51

Tumors identified in mice that were examined pathologically. The neural crest tumors were further classified as soft tissue sarcoma, pheochromocytoma, or neuroblastoma/paraganglioma. *The myeloid disorders identified included MPD (n = 9), MDS (n = 1), AML (n = 3), histiocytic sarcoma (n = 1), and refractory cytopenia with splenomegaly (n = 3). Two additional *Nf1*$^{+/-}$ mice with massive splenomegaly (>1 g) but no other gross abnormalities were not classified as having a myeloid malignancy as the cause of death.

Table 2. Tumors in *Nf1*$^{+/-}$ mice according to treatment group

Tumor type	Untreated (n = 12)	CY (n = 14)	RAD (n = 31)	CY + RAD (n = 29)	Latency (range in days)
Neural crest tumors	2	3	5	6	
Soft tissue sarcomas	0	2	2	4	172–469
Pheochromocytomas	1	1	2	2	382–494
Neuroblastoma/paraganglioma	1	0	1	0	467
Myeloid malignancies	2	1	10	4	215–519
Poorly differentiated tumors	0	1	1	1	389–410
Breast cancer	0	0	0	4	308–389
Other	1	1	4	5	158–467
Total	5	6	20	20	158–519

Tumors developing in *Nf1* mutant mice were subdivided according to exposure to radiation (RAD), cyclophosphamide (CY), or both modalities (RAD + CY), and the number of mice assigned to each group is also shown. The corresponding numbers of wild-type mice were as follows: control (n = 20), RAD (n = 32), CY (n = 17), and RAD + CY (n = 37). The neural crest tumors were further subclassified as soft tissue sarcoma, pheochromocytoma, or neuroblastoma/paraganglioma. Latency refers to the number of days from RAD treatment to when a tumor was detected. The mean latency was the same in mice that developed soft tissue sarcomas (359 days), myeloid malignancies (347 days), or breast cancer (341 days).

tent with epithelial origin. The histology of these breast cancers was remarkably uniform between cases. In general, areas of adenocarcinoma in situ were identified adjacent to infiltrating ductal carcinoma with both glandular and more solid growth patterns. The invasive component demonstrated high-grade nuclear features and abundant mitotic activity (>20 mf/10 hpf). Most of the breast cancers invaded into the underlying skeletal muscle. Overall, the pathologic features of these murine breast cancers were very similar to those of high-grade adenocarcinoma of the breast in humans.

Three *Nf1*$^{+/-}$ mice developed poorly differentiated malignant tumors that could not be characterized with precision. In addition, we incidentally detected benign bronchiolo/alveolar adenomas in the lungs of many older wild-type and *Nf1*$^{+/-}$ mice. Similar findings have been reported in other mouse strains (Dixon and Maronpot, 1991). These lesions were excluded from the analysis of malignancies, with the exception that six very large lung tumors (four in treated wild-type mice and two in treated *Nf1*$^{+/-}$ mice) that resulted in premature death were classified as malignant. Other tumor types noted included lymphoma (four wild-type, five *Nf1*$^{+/-}$), Harderian gland (three wild-type, two *Nf1*$^{+/-}$), osteosarcoma (two wild-type), and liver (one *Nf1*$^{+/-}$). Most of the wild-type and *Nf1*$^{+/-}$ mice that developed these tumors were exposed to CY, RAD, or both.

CGH analysis of primary tumors and tumor-derived cell lines

We performed CGH on primary sarcomas and breast cancers to identify copy number changes that might contribute to tumorigenesis. These studies uncovered multiple genomic changes

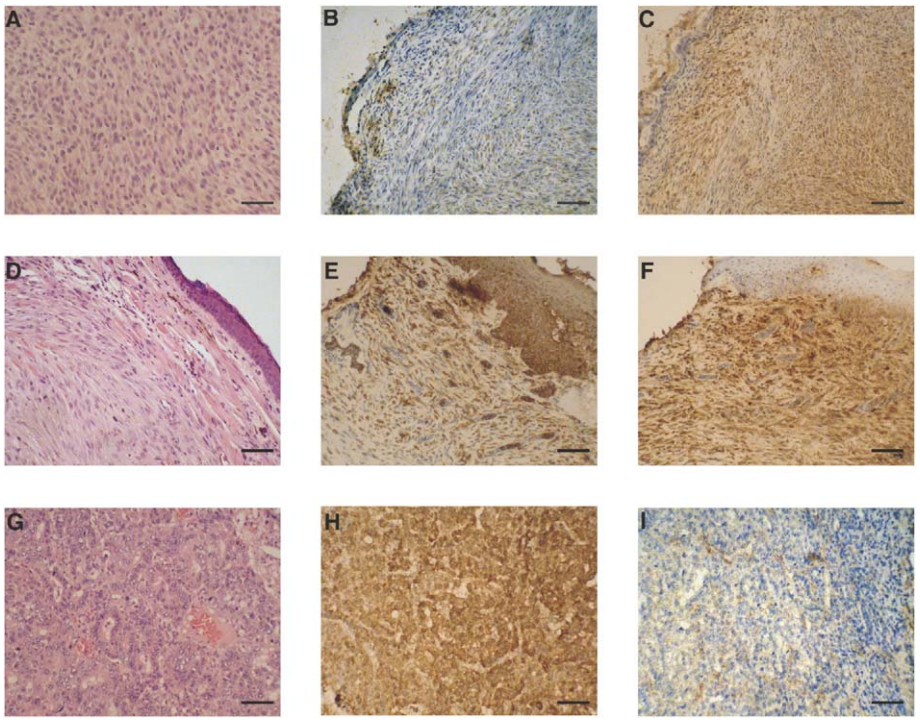

Figure 2. Histologic and immunocytochemical analysis of malignant tumors from *Nf1*$^{+/-}$ mice

Tumor tissues were stained with hematoxylin and eosin (**A**, **D**, and **G**), cytokeratin (CK; **B**, **E**, and **H**), or S100 (**C**, **F**, and **I**). **A**–**C** depict a spindle cell tumor from an *Nf1* mutant mouse that was exposed to CY and RAD. Immunohistochemical staining for CK was negative, while staining for S100 revealed intense cytoplasmic staining of a large proportion of spindle cells. **D**–**F** are sections of a spindle cell neoplasm from an *Nf1*$^{+/-}$ that was exposed to RAD. This tumor displayed positive staining for both CK and S100, with islands of CK-positive cells found in a background of predominantly S100-positive cells. **G**–**I** are from a breast adenocarcinoma that developed in a female *Nf1*$^{+/-}$ mouse exposed to both CY and RAD. This tumor displayed staining for CK but not S100. The scale bars are 50 μm in length.

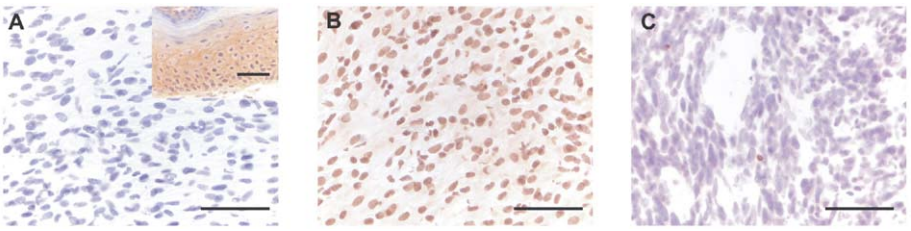

Figure 3. EGFR, p21, and p16 staining of genotoxin-induced sarcomas

A: A sarcoma section stained with an anti-EGFR antibody is negative for surface EGFR expression, while skin from the same mouse shows positive staining in the epidermis (insert).

B: Staining with an antibody against p21 demonstrates nuclear staining of the tumor cells.

C: A section stained with anti-p16 antibody is negative for staining in tumor cells. Note the positive staining seen in rare infiltrating leukocytes.

The scale bars are 50 μm in length.

in four of six sarcomas and in all of the breast cancers (see Table S1). Two independent clustering methodologies were employed to classify four sarcomas and four breast cancers that developed in mice exposed to CY + RAD based on their genomic profiles (see the Experimental Procedures). Both approaches led to a perfect separation of the sarcomas from the breast tumors (Figure 4). To evaluate the relative similarities of individual tumors grouped within each cluster, we performed within sum of squares analyses and found that this difference for breast tumors was less than half of that for the sarcomas. These results demonstrate that the genomic profiles of the breast cancers and sarcomas are distinct and that unsupervised approaches are capable of separating them into two groups, with the breast tumors showing a higher degree of similarity than the sarcomas. We were able to establish stable cell lines from four genotoxin-induced tumors that developed in *Nf1*$^{+/-}$ mice. Three were derived from breast cancers, and the fourth was from a soft tissue sarcoma. When we included these cell lines and performed hierarchical clustering analysis as before, the separation between breast cancers and sarcomas was preserved, and each cell line clustered together with the corresponding primary tumor with the exception of breast cancer B1 and cell line B1CL (Figure 4).

LOH at the *Nf1* and *Trp53* loci in tumors from *Nf1*$^{+/-}$ mice

Molecular investigation of tumors that develop spontaneously in persons with NF1 and in strains of *Nf1* mutant mice frequently demonstrates somatic loss of constitutional heterozygosity (Jacks et al., 1994b; Side and Shannon, 1998). Similarly, Southern blot analysis showed loss of the wild-type C57Bl/6 *Nf1* allele in six of eight soft tissue sarcomas, confirming the important role of biallelic inactivation of *Nf1* in tumorigenesis (Figure 5A). We also observed LOH in three of three pheochromocytomas and in four of four breast cancers. By contrast, polymerase chain reaction (PCR) genotyping did not reveal LOH in any of the myeloid malignancies.

Inactivation of *Trp53* and *Nf1* cooperate in tumorigenesis, particularly sarcoma development (Cichowski et al., 1999; Vogel et al., 1999). The loci for these two genes are approximately 7 cM apart on mouse chromosome 11, whereas the human homologs are separated by approximately 22 Mb on chromosome 17. We assayed the D11Mit29 polymorphic microsatellite marker, which is tightly linked to the *Trp53* locus, to determine if *Trp53* and *Nf1* are coordinately lost in malignancies that arise after mutagen exposure. Surprisingly, while LOH occurred in each of the breast tumors and in some pheochromocytomas, all of the sarcomas that developed in *Nf1*$^{+/-}$ mice retained both *Trp53* alleles (Figure 5B).

Chromosome 11 demonstrated copy number losses spanning the *Nf1* locus in all of the breast cancers and in two of the sarcomas (Figure 5C). Each tumor with copy number loss showed LOH at *Nf1.* While these data exclude amplification of

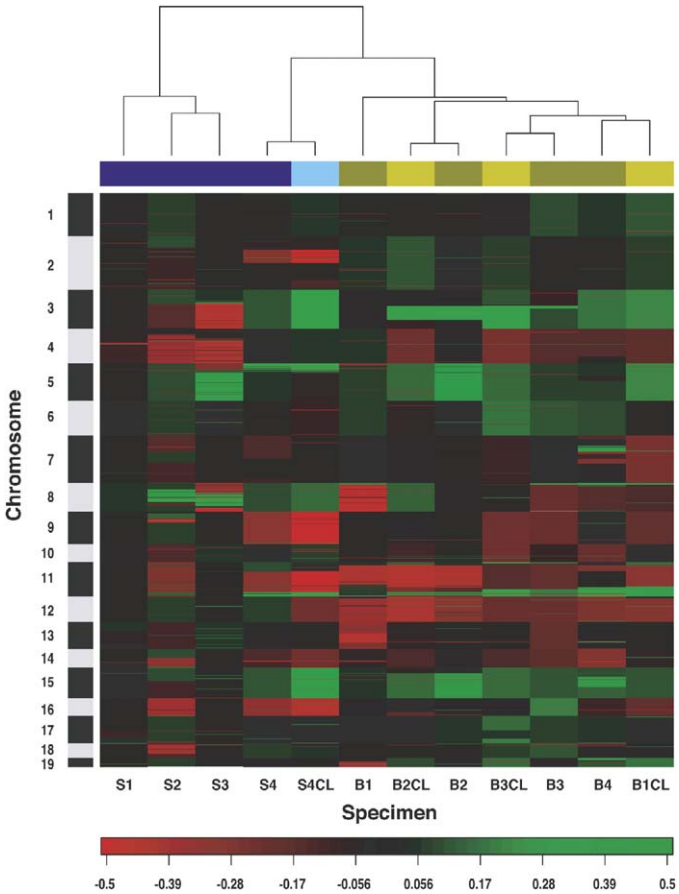

Figure 4. Hierarchical clustering of CGH data generated from SMNs and tumor cell lines in *Nf1* mice

The sarcomas are labeled "S1," "S2," "S3," and "S4" and are shown in dark blue; the sarcoma cell line is labeled "S4CL" and is shown in light blue; the breast cancers are labeled "B1," "B2," "B3," and "B4" and are shown in dark green; and the corresponding breast cancer cell lines are labeled "B1CL," "B2CL," and "B3CL" and are shown in light green. A red-to-green scale indicates the relative change in copy number, with losses shown in red and gains shown in green. The sarcomas and breast cancers form distinct clusters, and the cell lines are closely related to the primary tumors from which they were derived. Note the shared pattern of genomic changes within each tumor type (e.g., all of the breast cancers and cell lines show copy number reductions spanning chromosome 12).

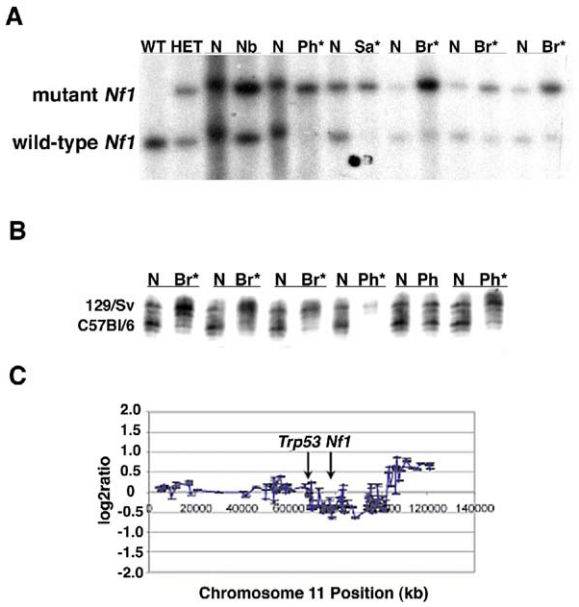

Figure 5. Molecular analysis at the *Nf1* and *Trp53* loci

A: Representative data from Southern blot analysis of tumors from *Nf1* mutant mice using a probe that distinguishes the wild-type (WT) and mutant *Nf1* alleles. Lanes 1 and 2 show analysis of normal tissues from wild-type and heterozygous *Nf1* mutant (HET) mice. The remaining lanes show paired normal (N) and tumor tissues from $Nf1^{+/-}$ mice that developed neuroblastoma (Nb), pheochromocytoma (Ph), sarcoma (Sa), or breast cancer (Br). Asterisks denote tumors with loss of the wild-type C57Bl/6 *Nf1* allele. Overall, 14 of 18 solid tumors that developed in $Nf1^{+/-}$ mutant mice showed loss of the normal *Nf1* allele (includes data not shown).

B: Representative data from analysis at the *Trp53* locus with the microsatellite marker D11Mit29 showing paired normal tissue (N) with tumor specimens from mice with breast cancer (Br) or pheochromocytoma (Ph). Tumors with LOH are marked with an asterisk. Whereas LOH was detected consistently in the breast cancers and was seen in most of the pheochromocytomas, it was uncommon in the sarcomas (data not shown). In each tumor with LOH, the *Trp53* allele was deleted from the C57Bl/6 chromosome, which carries a normal *Nf1* allele in *cis*.

C: Copy number gains and losses across chromosome 11 in sarcoma S4 that showed LOH at *Nf1* but retained two alleles at *Trp53*. The CGH data reveal reduced copy number spanning a DNA segment that includes *Nf1*, but not *Trp53*.

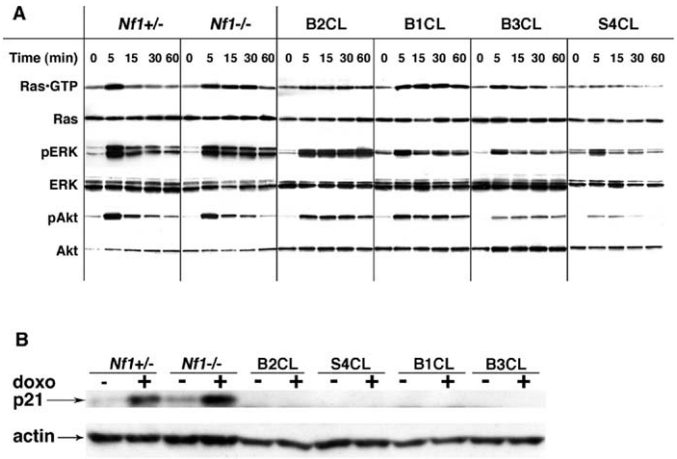

Figure 6. Biochemical analysis of MEFs and tumor cell lines developed from $Nf1^{+/-}$ mice

A: EGF induces a transient spike in Ras-GTP levels in $Nf1^{+/-}$ MEFs, which is followed by a rapid return to baseline values. By contrast, $Nf1^{-/-}$ MEFs show a sustained Ras-GTP response and prolonged ERK phosphorylation. Three breast cancer cell lines also show prolonged Ras-GTP levels as well as prolonged ERK and Akt phosphorylation.

B: Doxorubicin induces p21 expression in heterozygous and homozygous *Nf1* mutant MEFs. By contrast, p21 was not detected in any of the cell lines before or after doxorubicin exposure.

the mutant *Nf1* allele in tumor tissues, none of the copy number changes in the *Nf1* or *Trp53* regions is equivalent to a single-copy loss in a diploid cell. This could be due to the presence of some normal cells admixed with the tumor samples or, alternatively, to loss of the normal C57Bl/6 allele with duplication of the 129/Sv chromosome in a polyploid tumor genome with duplication of the 129/Sv chromosome.

Biochemical characterization of tumor cell lines

Based on previous data implicating aberrant EGFR signaling in NF1-associated sarcomagenesis (DeClue et al., 2000; Li et al., 2002), we compared EGF-induced activation of Ras and phosphorylation of the downstream effectors MEK and Akt in the four cell lines derived from genotoxin-induced cancers. Mouse embryonic fibroblasts (MEFs) were assessed in parallel. $Nf1^{+/-}$ MEFs that were plated, serum starved, and stimulated with EGF displayed a marked increase in Ras-GTP levels with a rapid return to baseline levels (Figure 6A). By contrast, $Nf1^{-/-}$ MEFs showed slightly higher peak levels of Ras-GTP in response to EGF and demonstrated prolonged Ras activation, which is consistent with a previous report (Cichowski et al., 2003). Levels of phosphorylated ERK and Akt changed in parallel with Ras-GTP. While there was some variability among the three breast cancer cell lines with respect to the degree and duration of Ras-GTP, ERK, and Akt activation, all of these cell lines showed elevated Ras-GTP levels for at least 30 min after EGF stimulation and persistence of phosphorylated Akt and ERK above baseline levels for 60 min (Figure 6A). By contrast, basal and EGF-induced Ras activation showed no consistent differences between the one sarcoma cell line and control $Nf1^{+/-}$ MEFS (Figure 6A).

We also compared the functional status of the p53 damage response pathway in MEFs and in tumor cell lines. *Nf1* mutant MEFs induced p21 expression in response to either doxorubicin (Figure 6B) or 5 Gy of RAD, which is expected in cells with an intact p53 pathway. The three breast cancer cell lines demonstrated LOH at the *Trp53* locus, whereas the sarcoma line retained both *Trp53* alleles. Each tumor cell line had high basal p53 expression, which is commonly associated with expression of mutant proteins, and failed to induce p21 in response to either doxorubicin (Figure 6B) or RAD (data not shown).

Discussion

Therapy-induced cancers are an increasing concern as more patients are surviving after receiving intensive regimens to treat a primary malignancy (Armitage et al., 2003; Bhatia and Sklar, 2002; Curtis et al., 1992; Kushner et al., 1998; Matesich and

Shapiro, 2003; Neglia et al., 1991; Smith et al., 2003; Tucker et al., 1988; van Leeuwen et al., 1994). Molecularly targeted therapeutics are appealing in principle as an alternative to genotoxic agents; however, the paucity of tractable biochemical targets and the frequent occurrence of de novo and acquired resistance imply that RAD and conventional chemotherapy will remain mainstays of therapeutic protocols for the foreseeable future. The experience in childhood cancers, where survival rates of ~75% have been achieved through the use of intensive chemotherapy and/or RAD, illustrates that success in curing primary cancers is associated with an increased incidence of SMNs (Bhatia and Sklar, 2002; de Vathaire et al., 1989a, 1989b). Unfortunately, the long-term toxicity of a therapeutic regimen may only become apparent years after many patients have been treated. Given these considerations, tractable animal models of SMN would be valuable for comparing the mutagenic potential of specific agents, for uncovering mechanisms of DNA damage in vivo, and for evaluating prevention strategies.

SMNs are problematic to model accurately in animals because the causative mutations result from exposure to genotoxins. By contrast, conventional strategies for generating tumor-prone mice involve engineering cancer-associated mutations into the germline. Although this is a powerful approach for investigating biologic effects of known therapy-related mutations such as *MLL* gene fusions in epipodophyllotoxin-induced leukemias (Dobson et al., 1999), introducing these cancer-associated mutations into the germline does not recapitulate the dynamic interaction between mutagen exposure and the host genome that underlies tumorigenesis. However, exposing wild-type mice to various doses and combinations of genotoxins is an inefficient and nonselective strategy for generating SMNs. The sensitized genetic background of *Nf1*$^{+/-}$ mice allowed us to develop a tractable and penetrant model of common SMNs that affect human patients. Moreover, the highly significant increase in tumor formation in *Nf1* mutant mice and the frequent loss of the normal *Nf1* allele in genotoxin-induced tumors reveals a direct mechanistic interaction between mutagen exposure and somatic mutations at this locus.

Myeloid malignancies and sarcomas were the most common SMNs detected in *Nf1*$^{+/-}$ mice. These data are consistent with observations in NF1 patients and, importantly, represent two of the most common sporadic SMNs (Armitage et al., 2003; Bhatia and Sklar, 2002; Matesich and Shapiro, 2003; Smith et al., 2003). We previously found that CY cooperates with heterozygous loss of *Nf1* to increase the incidence of MPD, with a substantially higher penetrance in inbred 129/Sv strain mice than in F1 129/Sv × C57Bl/6 animals (Mahgoub et al., 1999). Genetic analysis of bone marrow and splenic DNA from mice with MPD revealed a higher frequency of LOH at *Nf1* in the 129/Sv background. The genetic mechanism, which involves deletion of the normal *Nf1* allele and duplication of the mutant allele (Mahgoub et al., 1999), is also seen in most of the myeloid malignancies that arise in patients with NF1 (K. Stephens, M.M. Le Beau, and K.M.S., unpublished data). Based on these results, we speculate that the low rate of myeloid malignancies that we observed in CY-treated mice is due to the F1 strain background and might be related to a reduced rate of mitotic recombination between 129/Sv and C57Bl/6 chromosome 11 homologs. In the current study, we investigated F1 mice to increase the probability of obtaining nonhematologic cancers and to induce tumors that were heterozygous at multiple genetic loci. It is striking that exposing *Nf1*$^{+/-}$ mice to RAD or to the combination of RAD + CY induced a wide spectrum of myeloid disorders, including refractory cytopenias, MDS, and AML, whereas control and CY-treated *Nf1*$^{+/-}$ mice almost always develop MPD (Mahgoub et al., 1999). Similarly, Japanese atomic bomb survivors are predisposed to chronic myeloid leukemia (CML), AML, and MDS (Imamura et al., 2002; Preston et al., 1994), and patients who are treated with alkylating agents and/or RAD develop both MDS and AML (Armitage et al., 2003; Le Beau et al., 1986; Thirman and Larson, 1996). Because MDS can be difficult to diagnose in both humans and mice, we may have underestimated the incidence of myeloid malignancies by excluding two mice that died with splenomegaly without a definitive diagnosis. Although the number of animals assigned to each treatment group is too small to compare individual regimens, there is no evidence that RAD and CY cooperate in this model, and our data raise the intriguing possibility that RAD may be more leukemogenic than RAD + CY. One potential explanation for this apparent paradox is that the probability of a mutant leukemia-initiating cell surviving and inducing disease in vivo might be higher after RAD only if the combination of CY + RAD induces severe DNA damage that results in cell death or senescence. It is interesting that we did not detect LOH at *Nf1* in bone marrow from mice that developed myeloid malignancies, which contrasts with the solid tumors. Similarly, five therapy-induced human leukemias from NF1 patients retained both alleles (Maris et al., 1997). It is possible that the wild-type *Nf1* allele is inactivated by point mutations or other subtle alterations in humans and mice; alternatively, genotoxin-induced mutations may cooperate with haploinsufficiency at the *Nf1* locus in the F1 genetic background. Consistent with this hypothesis, heterozygous inactivation of *Nf1* has phenotypic consequences in mast cells and melanocytes (Ingram et al., 2000), and therapy-related myeloid malignancies from NF1 patients demonstrate acquired chromosomal abnormalities such as monosomy 7 (Maris et al., 1997; Papageorgio et al., 1999).

In addition to inducing myeloid malignancies, RAD is strongly associated with subsequent development of sarcomas within the RAD portals of patients treated for nonmalignant diseases and for a variety of cancers (Beck, 1922; Boice et al., 1988; Darby et al., 1987; Doherty et al., 1986; Halperin et al., 1984; Marsche, 1922; Murray et al., 1999; Pendlebury et al., 1995; Smith and Doll, 1982). Many of these tumors are high-grade osteosarcomas or malignant fibrous histiocytomas that have a poor prognosis (Huvos et al., 1985; Inwards and Unni, 1995; Laskin et al., 1988; Murray et al., 1999). Although *TP53* inactivation is common in RAD-induced sarcomas (Brachman et al., 1991; Nakanishi et al., 1998), the other molecular lesions are largely unknown (Beech et al., 1998; Cowan et al., 1990; Remmelink et al., 1998; Sekyi-Otu et al., 1995; Wang et al., 1994). MPNST, the most common sarcoma that arises de novo in persons with NF1, has also been reported as a SMN (Li et al., 2002). MPNSTs typically display complex karyotypes and may also show loss of the normal *NF1* allele, mutations that deregulate the pRb and p53 pathways, and aberrant expression of EGFR (Birindelli et al., 2001; DeClue et al., 2000; Halling et al., 1996; Liapis et al., 1999; Plaat et al., 1999). A few small studies of human RAD-induced sarcomas have suggested the existence of nonrandom cytogenetic aberr-

ations including translocation breakpoints involving chromosome band 1p13 and 7p22, gain of 7q1, and losses of 9p2, 1p3, and 21p1-q2 (Bridge et al., 2004; Mertens et al., 1995; Plaat et al., 1999). Human chromosome band 7q1 is orthologous to two segments of mouse chromosome 5. Interestingly, our CGH analysis revealed a discrete region of amplification in four of six sarcomas and in the four breast cancers at BAC RP23-281N22, which is within the segment of mouse chromosome 5 that is syntenic to human 7q1. This BAC includes a number of putative genes including a homolog of the *Drosophila* frizzled gene, a FK506 binding protein, and a putative zinc finger transcription factor. We also identified a region of amplification on mouse chromosome 8 in breast cancer samples that corresponds to an interval of human chromosome 13q34 that is amplified in hepatocellular carcinoma and some other epithelial cancers (Yasui et al., 2002). This segment includes the *TFDP1*, *CUL4A*, and *CDC16* genes.

Two groups crossed *Nf1* and *Trp53* mutant mice to generate recombinant founders that carried both mutant alleles on the same chromosomal homolog (i.e., in *cis* configuration) in order to recapitulate the simultaneous loss of *NF1* and *TP53* frequently seen in NF1-associated MPNSTs. Whereas heterozygous and homozygous *Trp53* mutant mice spontaneously develop tumors (primarily lymphomas) at 30–50 weeks of age (Donehower et al., 1992; Jacks et al., 1994a), many *cis* and *trans* $Nf1^{+/-};Trp53^{+/-}$ mice developed early-onset sarcomas that resembled human MPNSTs. Molecular analysis revealed LOH at both *Nf1* and *Trp53* in at least 70% of the soft tissue tumors from *cis* $Nf1^{+/-};Trp53^{+/-}$ mice. Based on these data, we were surprised that RAD- and CY-induced sarcomas with LOH at *Nf1* generally retained both *Trp53* alleles. Residual p53 function may underlie the failure of most of these tumors to grow as permanent cell lines, which is in contrast to sarcomas from *cis* $Nf1^{+/-};Trp53^{+/-}$ mice (L. Parada, personal communication). In this regard, it is of interest that the sarcoma cell line that we obtained had abnormal p53 pathway function as assessed by elevated p53 expression and failure to induce p21 in response to RAD and doxorubicin. Although we cannot exclude similar defects in other RAD- and CY-induced tumors, our data suggest the existence of one or more p53-independent pathways to sarcoma development. This hypothesis is consistent with studies of NF1-associated de novo MPNSTs, which uncovered either LOH at *TP53* or a somatic mutation in less than half of the tumors (Birindelli et al., 2001; Halling et al., 1996; Lothe et al., 2001; Menon et al., 1990). Aberrant expression of the EGF receptor has also been implicated in the development of MPNST in humans and in mouse models (DeClue et al., 2000; Li et al., 2002; Ling et al., 2005), and a recent study demonstrated that reducing EGFR signaling by ~90% dramatically reduced the incidence of sarcoma in *cis* $Nf1^{+/-};Trp53^{+/-}$ mice (Ling et al., 2005). By contrast, none of the genotoxin-induced soft tissue tumors that developed in $Nf1^{+/-}$ mice expressed detectable level of EGFR. These data are consistent with the observation that ~30% of MPNSTs from NF1 patients do not express EGFR mRNA (Watson et al., 2004). The expression profiles of this subset of tumors were characterized by elevated levels of neuroglial markers and by relatively low expression of transcripts that are associated with proliferation. Together, our molecular and immunohistochemical data support a distinct pathway of genotoxin-induced sarcomagenesis that involves loss of *Nf1*, normal p53 activity, and a lack of EGFR amplification. The recurring copy number changes detected by CGH analysis of these tumors imply that limited numbers of cooperating events promote clonal outgrowth in vivo.

The observation that female $Nf1^{+/-}$ mice developed breast cancer after exposure to RAD or RAD in combination with CY was unexpected and intriguing. The incidence of SMNs has been investigated over many decades in patients who were treated for Hodgkin's disease as adolescents or young adults. Among these individuals, breast cancer is the most common solid SMN in women, with a cumulative probability of up to 42% after 30 years (Bhatia et al., 1996). Although RAD dose, combined treatment with chemotherapy, and age at the time of treatment strongly influence the risk of subsequent development of secondary breast cancer, the genetic pathways that underlie malignant transformation are poorly understood. CGH analysis of these tumors uncovered a striking pattern of recurring copy number changes involving chromosome 12 and other DNA segments (Figure 3 and Supplemental Data). Together, our data imply that loss of *Trp53* and hyperactive Ras cooperate with a common series of secondary genetic changes in mammary tumorigenesis after genotoxin exposure.

Hyperactivation of the PI3 kinase/Akt cascade underlies growth factor-independent survival in immortalized *Nf1*-deficient hematopoietic cells, whereas aberrant MAP kinase signaling drives proliferation and autocrine production of granulocyte-macrophage colony stimulating factor (GM-CSF) (Donovan et al., 2002a). In addition, recent studies in *Nf1*-deficient astrocytes and MEFs have uncovered deregulated activation of S6 kinase, a downstream effector of mTOR (Dasgupta et al., 2005; Johannessen et al., 2005). Dephosphorylation of tuberin (the protein encoded by the *TSC2* tumor suppressor gene) by activated Akt is an important mechanism that contributes to hyperactive mTOR/S6 kinase in *Nf1*-deficient cells (Johannessen et al., 2005). We found that breast cancer cell lines from $Nf1^{+/-}$ mice responded to EGF with prolonged activation of Ras, ERK, and Akt, and it will be of interest to determine how this modulates the activation status of downstream effectors and contributes to specific cellular phenotypes. Based on the data of Li and colleagues (Li et al., 2002) showing elevated levels of EGFR expression in most sarcoma cell lines from *cis* $Nf1^{+/-};Trp53^{+/-}$ mice, we investigated signaling in response to EGF in the S4CL cell line. The modest increase in ERK phosphorylation that we observed in response to EGF is consistent with our data showing that sarcomas that arise in $Nf1^{+/-}$ mice that are exposed to genotoxins do not express detectable levels of EGFR.

$Nf1^{+/-}$ mice are a robust and tractable in vivo system that can be harnessed to address the mutagenic potential of cancer treatments and to test preventive strategies. This "first generation" model can also be refined further; for example, it is feasible to selectively administer a range of RAD doses to the mammary glands of mice, and to test how age, previous pregnancies, and hormonal manipulations modulate tumorigenesis. A more challenging experimental question involves investigating if the therapy-induced cancers that develop in this model are largely refractory to conventional chemotherapeutic agents, and if this is true, this model may prove useful for testing novel therapeutic strategies. Unlike hematopoietic cancers, there are no simple techniques for transplanting primary solid tumors into immunocompetent recipients, which would greatly facilitate studies of this nature. Our data also have implications for

treating tumors that arise in the patients with NF1. In particular, we found that a single low dose of RAD cooperated strongly with heterozygous *Nf1* inactivation in tumorigenesis. Children with NF1 are predisposed to optic track gliomas and low-grade astrocytomas, which may be difficult to manage. Our data suggest that the potential risk of SMN should be considered when deciding whether to irradiate these and other NF1-associated tumors and that patients who require RAD should be followed carefully for subsequent treatment-induced cancers.

Experimental procedures

Mouse stains, breeding, and treatment

All experimental procedures involving mice were reviewed and approved by the UCSF Committee on Animal Research. Heterozygous *Nf1* mutant mice that were maintained in the 129/Sv strain background (Jacks et al., 1994b) were mated with wild-type C57Bl/6 mice (Jackson Labs, Bar Harbor, ME) to generate wild-type and $Nf1^{+/-}$ mice. These mice were genotyped and assigned to one of the four experimental groups. Study mice were housed in a pathogen-free environment at the UCSF Animal Care Facility. Mice exposed to CY (Mead Johnson Oncology Products) received intraperitoneal injections of CY (200 mg/ml in sterile water) medial to the proximal aspect of the femur. RAD-treated mice received a single dose of 3 Gy, which was administered using a cesium-137 source (JL Shepherd & Associates, San Fernando, CA) at a rate of ~250 cGy/min.

Pathologic analysis

Complete blood counts (CBCs) were measured on blood samples taken premortem from tail vein bleeding and postmortem by intracardiac puncture in Hema-Vet 850 hematology analyzer (CDC Technologies, Inc., Oxford, CT). Blood and bone marrow smears were made on glass slides, and cytospin slides were prepared by suspending 100,000 viable cells in 200 μl of PBS and centrifuging them for 10 min at 400 rpm. The slides were stained with Wright-Giemsa (Fisher) and examined using a Nikon Eclipse E400 microscope. Tumor tissues were fixed in 10% formalin (Fisher) and embedded in paraffin, cut, and stained with hematoxylin and eosin. Slides of tumor tissues were stained with antibodies against CK and S100 (Dako, Carpinteria, CA) according to the manufacturer's instructions. EGFR expression, p16 expression, and p21 expression were assessed on 10 μm thick cryostat sections cut from frozen tumor specimens. Briefly, the slides were fixed in cold acetone or 4% paraformaldehyde and then blocked with serum followed by incubation with avidin then biotin blocking reagents (Vector Laboratories). Sections were immunostained using standard procedures with rabbit antibodies against EGFR (SC-03), p16 (SC-1207), and p21 (SC-397) (Santa Cruz Biotechnology) and enhanced with ABC Elite Vector Stain Substrate Kit (Vector Laboratories) using the manufacturer's protocol. Staining was visualized with 3,3′-diaminobenzidine (DAB Substrate Kit, Vector Laboratories) and counterstained with Gill's hematoxylin (Santa Cruz Biotechnology). Blood, bone marrow, and spleen sections from mice with hematopoietic malignancies were reviewed by a hematopathologist with expertise in murine myeloid malignancies (S.C.K.). A veterinary pathologist with experience in evaluating mouse cancer models (A.B.) and a pathologist with expertise in human sarcomas (A.H.) independently reviewed the solid tumor slides.

Genotyping and mutation analysis

Mice were genotyped at the *Nf1* locus, and LOH was performed on solid tumor specimens using Southern blot analysis as described elsewhere (Jacks et al., 1994b). A PCR-based assay was employed to assess myeloid malignancies for LOH at *Nf1*. LOH analysis was performed at the D11Mit29 locus amplifying tumor DNA samples with 3′ and 5′ γ-^{33}P-labeled primers (Research Genetics, Carlsbad, CA). The amplification products were resolved on a polyacrylamide gel and visualized by autoradiography.

Cell culture

Cells were maintained at 37°C in humidified incubator with 5% CO_2. To generate tumor cell lines, a 10–100 mm^3 piece tissue was first washed with Dulbecco's modified essential medium (DMEM) containing penicillin and streptomycin and minced with a sterile scalpel. After adding 2–3 ml of DMEM with 10% FBS (Hyclone, Logan, UT), the tissue was passed through a 16G needle (Becton-Dickinson, Franklin Lakes, NJ), plated in two wells of a six-well plate (Corning, Corning, NY), and cultured at 37°C. The medium was changed every 1–3 days, and cells that proliferated in culture were trypsinized, passaged, and frozen. MEFs were generated from E13.6 F1 embryos by first dissecting the fetal liver and head, and then mincing and trypsinizing the remaining tissues, and culturing the cells in DMEM supplemented with 10% FBS, glutamine, and β-mercaptoethanol (Sigma, St. Louis, MO).

Acquisition and analysis of CGH data

Array CGH was carried out on arrays of 2500 mouse BACs as described previously (Snijders et al., 2005). Briefly, test and reference DNA samples from 129/Sv × C57Bl/6 female F1 mice were labeled by random priming to incorporate Cy3- and Cy5-dUTP, respectively. The labeled DNAs together with Cot-1 DNA (Invitrogen) were hybridized to the arrays for 48 hr. Following washing 16 bit 1024 × 1024 pixel DAPI, Cy3 and Cy5 images were collected with a custom-built CCD camera system as described previously (Pinkel et al., 1998). "UCSF SPOT" software (Jain et al., 2002) was used to automatically segment the spots based on the DAPI images, perform local background correction, and calculate various measurement parameters, including log2 ratios of the total integrated Cy3 and Cy5 intensities for each spot. A second custom program, SPROC, was used to obtain averaged ratios of the triplicate spots for each clone, standard deviations of the triplicates, and plotting position for the BACs on the May 2004 freeze of the mouse genome sequence (http://genome.ucsc.edu/). Data files were edited to remove ratios on clones for which only one of the triplicates remained after SPROC analysis and/or the standard deviation of the log2 ratios of the triplicates was >0.2.

To address the distinction between types of tumors based on their genomic profiles, we applied clustering approaches (Fridlyand et al., 2004). The clones missing in more than 20% of the samples were filtered out, and each sample was segmented using DNA copy (Olshen et al., 2004). The tumor-specific experimental error was estimated as median absolute deviation (MAD) of the differences between the observed log2 ratios and the means of their corresponding segments. The clones with log2 ratios further away from their segment mean than 4 × MAD retained their original log2 ratios, whereas the rest of the clones were assigned the value of their segment mean. The distance between a pair of samples was computed as 1 – Pearson correlation calculated over the autosomal clones. The resulting distance matrix was used as an input to hierarchical (see Figure 3) and k-means clustering with two groups. To evaluate the relative similarity of the two clusters we compared the within sum of squares of each cluster, which is an output of the k-means procedure in the R statistical package.

Biochemical analysis

Cell lines or MEFs were plated a density of 1.5–2 × 10^6 cells per 10 cm plate in DMEM with 10% FBS. After 16–20 hr, the cells were washed and transferred to DMEM without serum. After 24 hr, the cells were stimulated with EGF (Peprotech, Rocky Hill, NJ) at 10 ng/ml for 5–60 min. The cells were lysed in Holstrom buffer, protein levels were quantified using the modified Bradford assay (Bio-Rad, Hercules, CA), and the samples were resolved using SDS-PAGE in 10%–12.5% precast gels (Bio-Rad). The proteins were transferred to an Immobilon filter (Amersham, Piscataway, NJ) and probed with antibodies labeled with horseradish peroxidase. The filters were incubated with ECL (Amersham) reagent and then exposed to film. We used the following primary antibodies to detect specific proteins: anti-pan-Ras antibody (Oncogene Research Products, San Diego, CA), anti-pERK (Santa Cruz Biotechnology, Santa Cruz, CA), anti-ERK antibody (Cell Signaling, Beverly, MA), anti-pAkt antibody (a kind gift from David Stokoe), anti-Akt antibody (Cell Signaling). Ras-GTP levels were quantified using an excess of Raf1 RBD-GST conjugated agarose beads (Upstate, Charlottesville, VA) according to the manufacturer's instructions. For studies of p53 function, cells that were irradiated to a dose of 5 Gy were incubated at 37°C for 3 hr or incubated with doxorubicin for approximately 16 hr. The cells were lysed, and Western blotting was performed as described above with antibodies that recognize p53 (Santa Cruz Biotechnology) and p21 (Santa Cruz Biotechnology).

Sample size and statistical analysis

The primary endpoint for statistical analysis was the effect of RAD, alone or in combination with CY, on the incidence of cancer in *Nf1*$^{+/-}$ mice. Based on previous data, we estimated the risk of tumor development in untreated F1 *Nf1*$^{+/-}$ mice to be 10% over 16 months. Since the primary goal was to examine if RAD cooperates with heterozygous *Nf1* inactivation in tumorigenesis, we allocated twice as many mice to the RAD cohorts in order to conserve resources.

Supplemental data

The Supplemental Data include two figures and one table and can be found with this article online at http://www.cancercell.org/cgi/content/full/8/4/337/DC1/.

Acknowledgments

We are grateful to Abigail Aiyagari, Charles Fezzie, Ben Yen, Robert Cardiff, Angell Shieh, and Doan Le for advice and for assisting with various aspects of this study. We are also indebted to David Stokoe, who provided the anti-pAkt antibody that we used in these studies. This work was supported by US Army Neurofibromatosis Research Program projects DAMD 17-02-1-0638 and DAMD17-98-1-8608, NIH grants R01 CA72614 and U01 CA84221, and the Jeffrey and Karen Peterson Family Foundation (all to K.M.S.); by NIH training grant T32ES07106 (R.C.C.); and by NIH grants U01 CA84118 and R01 CA101359 (D.G.A.). S.C.K. is a Scholar of the Leukemia and Lymphoma Society of America, and T.E.J. is an Investigator of the Howard Hughes Medical Institute.

Received: February 9, 2005
Revised: June 24, 2005
Accepted: August 26, 2005
Published: October 17, 2005

References

Armitage, J.O., Carbone, P.P., Connors, J.M., Levine, A., Bennett, J.M., and Kroll, S. (2003). Treatment-related myelodysplasia and acute leukemia in non-Hodgkin's lymphoma patients. J. Clin. Oncol. *21*, 897–906.

Beck, A. (1922). Zur Frage des Röntgensarkoms, Zugleich ein Beitrag zur Pathogenese des Sarkoms. Munch. Med. Wochenschr. *69*, 623–624.

Beech, D., Pollock, R.E., Tsan, R., and Radinsky, R. (1998). Epidermal growth factor receptor and insulin-like growth factor-I receptor expression and function in human soft-tissue sarcoma cells. Int. J. Oncol. *12*, 329–336.

Bhatia, S., and Sklar, C. (2002). Second cancers in survivors of childhood cancer. Nat. Rev. Cancer *2*, 124–132.

Bhatia, S., Robison, L.L., Oberlin, O., Greenberg, M., Bunin, G., Fossati-Bellani, F., and Meadows, A.T. (1996). Breast cancer and other second neoplasms after childhood Hodgkin's disease. N. Engl. J. Med. *334*, 745–751.

Birindelli, S., Perrone, F., Oggionni, M., Lavarino, C., Pasini, B., Vergani, B., Ranzani, G.N., Pierotti, M.A., and Pilotti, S. (2001). Rb and TP53 pathway alterations in sporadic and NF1-related malignant peripheral nerve sheath tumors. Lab. Invest. *81*, 833–844.

Boguski, M., and McCormick, F. (1993). Proteins regulating Ras and its relatives. Nature *366*, 643–653.

Boice, J.D., Jr., Engholm, G., Kleinerman, R.A., Blettner, M., Stovall, M., Lisco, H., Moloney, W.C., Austin, D.F., Bosch, A., Cookfair, D.L., et al. (1988). Radiation dose and second cancer risk in patients treated for cancer of the cervix. Radiat. Res. *116*, 3–55.

Brachman, D.G., Hallahan, D.E., Beckett, M.A., Yandell, D.W., and Weichselbaum, R.R. (1991). p53 gene mutations and abnormal retinoblastoma protein in radiation-induced human sarcomas. Cancer Res. *51*, 6393–6396.

Bridge, R.S., Jr., Bridge, J.A., Neff, J.R., Naumann, S., Althof, P., and Bruch, L.A. (2004). Recurrent chromosomal imbalances and structurally abnormal breakpoints within complex karyotypes of malignant peripheral nerve sheath tumour and malignant triton tumour: a cytogenetic and molecular cytogenetic study. J. Clin. Pathol. *57*, 1172–1178.

Cichowski, K., and Jacks, T. (2001). NF1 tumor suppressor gene function: Narrowing the GAP. Cell *104*, 593–604.

Cichowski, K., Shih, T.S., Schmitt, E., Santiago, S., Reilly, K., McLaughlin, M.E., Bronson, R.T., and Jacks, T. (1999). Mouse models of tumor development in neurofibromatosis type 1. Science *286*, 2172–2176.

Cichowski, K., Santiago, S., Jardim, M., Johnson, B.W., and Jacks, T. (2003). Dynamic regulation of the Ras pathway via proteolysis of the NF1 tumor suppressor. Genes Dev. *17*, 449–454.

Cowan, J.M., Beckett, M.A., Tarbell, N., and Weichselbaum, R.R. (1990). Symmetrical chromosome rearrangements in cell lines established from human radiation-induced sarcomas. Cancer Genet. Cytogenet. *50*, 125–137.

Curtis, R.E., Boice, J.D., Jr., Stovall, M., Bernstein, L., Greenberg, R.S., Flannery, J.T., Schwartz, A.G., Weyer, P., Moloney, W.C., and Hoover, R.N. (1992). Risk of leukemia after chemotherapy and radiation treatment for breast cancer. N. Engl. J. Med. *326*, 1745–1751.

Darby, S.C., Doll, R., Gill, S.K., and Smith, P.G. (1987). Long term mortality after a single treatment course with X-rays in patients treated for ankylosing spondylitis. Br. J. Cancer *55*, 179–190.

Dasgupta, B., and Gutmann, D.H. (2003). Neurofibromatosis 1: Closing the GAP between mice and men. Curr. Opin. Genet. Dev. *13*, 20–27.

Dasgupta, B., Yi, Y., Chen, D.Y., Weber, J.D., and Gutmann, D.H. (2005). Proteomic analysis reveals hyperactivation of the mammalian target of rapamycin pathway in neurofibromatosis 1-associated human and mouse brain tumors. Cancer Res. *65*, 2755–2760.

DeClue, J.E., Heffelfinger, S., Benvenuto, G., Ling, B., Li, S., Rui, W., Vass, W.C., Viskochil, D., and Ratner, N. (2000). Epidermal growth factor receptor expression in neurofibromatosis type 1-related tumors and NF1 animal models. J. Clin. Invest. *105*, 1233–1241.

de Vathaire, F., Francois, P., Hill, C., Schweisguth, O., Rodary, C., Sarrazin, D., Oberlin, O., Beurtheret, C., Dutreix, A., and Flamant, R. (1989a). Role of radiotherapy and chemotherapy in the risk of second malignant neoplasms after cancer in childhood. Br. J. Cancer *59*, 792–796.

de Vathaire, F., Schweisguth, O., Rodary, C., Francois, P., Sarrazin, D., Oberlin, O., Hill, C., Raquin, M.A., Dutreix, A., and Flamant, R. (1989b). Long-term risk of second malignant neoplasm after a cancer in childhood. Br. J. Cancer *59*, 448–452.

Dixon, D., and Maronpot, R.R. (1991). Histomorphologic features of spontaneous and chemically-induced pulmonary neoplasms in B6C3F1 mice and Fischer 344 rats. Toxicol. Pathol. *19*, 540–556.

Dobson, C.L., Warren, A.J., Pannell, R., Forster, A., Lavenir, I., Corral, J., Smith, A.J., and Rabbitts, T.H. (1999). The mll-AF9 gene fusion in mice controls myeloproliferation and specifies acute myeloid leukaemogenesis. EMBO J. *18*, 3564–3574.

Doherty, M.A., Rodger, A., and Langlands, A.O. (1986). Sarcoma of bone following therapeutic irradiation for breast carcinoma. Int. J. Radiat. Oncol. Biol. Phys. *12*, 103–106.

Donehower, L., Harvey, M., Slagle, B., McArthur, M., Montgomery, C., Butel, J., and Bradley, A. (1992). Mice deficient for p53 are developmentally normal but susceptible to spontaneous tumours. Nature *356*, 215–221.

Donovan, S., See, W., Bonifas, J., Stokoe, D., and Shannon, K.M. (2002a). Hyperactivation of protein kinase B and ERK have discrete effects on survival, proliferation, and cytokine expression in Nf1-deficient myeloid cells. Cancer Cell *2*, 507–514.

Donovan, S., Shannon, K.M., and Bollag, G. (2002b). GTPase activating proteins: critical regulators of intracellular signaling. Biochim. Biophys. Acta *1602*, 23–45.

Fridlyand, J., Snijders, A.M., Pinkel, D., Albertson, D.G., and Jain, A.N. (2004). Hidden Markov models approach to the analysis of array CGH data. J. Multivariate Anal., in press.

Halling, K.C., Scheithauer, B.W., Halling, A.C., Nascimento, A.G., Ziesmer, S.C., Roche, P.C., and Wollan, P.C. (1996). p53 expression in neurofibroma

and malignant peripheral nerve sheath tumor. An immunohistochemical study of sporadic and NF1-associated tumors. Am. J. Clin. Pathol. *106*, 282–288.

Halperin, E.C., Greenberg, M.S., and Suit, H.D. (1984). Sarcoma of bone and soft tissue following treatment of Hodgkin's disease. Cancer *53*, 232–236.

Hawkins, M.M., Draper, G.J., and Kingston, J.E. (1987). Incidence of second primary tumours among childhood cancer survivors. Br. J. Cancer *56*, 339–347.

Huvos, A.G., Woodard, H.Q., Cahan, W.G., Higinbotham, N.L., Stewart, F.W., Butler, A., and Bretsky, S.S. (1985). Postradiation osteogenic sarcoma of bone and soft tissues. A clinicopathologic study of 66 patients. Cancer *55*, 1244–1255.

Imamura, N., Abe, K., and Oguma, N. (2002). High incidence of point mutations of p53 suppressor oncogene in patients with myelodysplastic syndrome among atomic-bomb survivors: a 10-year follow-up. Leukemia *16*, 154–156.

Ingram, D.A., Yang, F.C., Travers, J.B., Wenning, M.J., Hiatt, K., New, S., Hood, A., Shannon, K., Williams, D.A., and Clapp, D.W. (2000). Genetic and biochemical evidence that haploinsufficiency of the Nf1 tumor suppressor gene modulates melanocyte and mast cell fates in vivo. J. Exp. Med. *191*, 181–188.

Inwards, C.Y., and Unni, K.K. (1995). Classification and grading of bone sarcomas. Hematol. Oncol. Clin. North Am. *9*, 545–569.

Jacks, T., Remington, L., Williams, B.O., Schmitt, E.M., Halachmi, S., Bronson, R.T., and Weinberg, R.A. (1994a). Tumor spectrum analysis in p53-mutant mice. Curr. Biol. *4*, 1–7.

Jacks, T., Shih, S., Schmitt, E.M., Bronson, R.T., Bernards, A., and Weinberg, R.A. (1994b). Tumorigenic and developmental consequences of a targeted *Nf1* mutation in the mouse. Nat. Genet. *7*, 353–361.

Jain, A.N., Tokuyasu, T.A., Snijders, A.M., Segraves, R., Albertson, D.G., and Pinkel, D. (2002). Fully automatic quantification of microarray image data. Genome Res. *12*, 325–332.

Johannessen, C.M., Reczek, E.E., James, M.F., Brems, H., Legius, E., and Cichowski, K. (2005). The NF1 tumor suppressor critically regulates TSC2 and mTOR. Proc. Natl. Acad. Sci. USA *102*, 8573–8578.

Kogan, S.C., Ward, J.M., Anver, M.R., Berman, J.J., Brayton, C., Cardiff, R.D., Carter, J.S., de Coronado, S., Downing, J.R., Fredrickson, T.N., et al. (2002). Bethesda proposals for classification of nonlymphoid hematopoietic neoplasms in mice. Blood *100*, 238–245.

Kushner, B.H., Heller, G., Cheung, N.K., Wollner, N., Kramer, K., Bajorin, D., Polyak, T., and Meyers, P.A. (1998). High risk of leukemia after short-term dose-intensive chemotherapy in young patients with solid tumors. J. Clin. Oncol. *16*, 3016–3020.

Laskin, W.B., Silverman, T.A., and Enzinger, F.M. (1988). Postradiation soft tissue sarcomas. An analysis of 53 cases. Cancer *62*, 2330–2340.

Le Beau, M.M., Albain, K.S., Larson, R.A., Vardiman, J.W., Davis, E.M., Blough, R.R., Golomb, H.M., and Rowley, J.D. (1986). Clinical and cytogenetic correlations in 63 patients with therapy-related myelodysplastic syndromes and acute nonlymphocytic leukemia: further evidence for characteristic abnormalities of chromosomes no. 5 and 7. J. Clin. Oncol. *4*, 325–345.

Li, F.P., and Fraumeni, J.F., Jr. (1982). Prospective study of a family cancer syndrome. JAMA *247*, 2692–2694.

Li, H., Velasco-Miguel, S., Vass, W.C., Parada, L.F., and DeClue, J.E. (2002). Epidermal growth factor receptor signaling pathways are associated with tumorigenesis in the Nf1:p53 mouse tumor model. Cancer Res. *62*, 4507–4513.

Liapis, H., Marley, E.F., Lin, Y., and Dehner, L.P. (1999). p53 and Ki-67 proliferating cell nuclear antigen in benign and malignant peripheral nerve sheath tumors in children. Pediatr. Dev. Pathol. *2*, 377–384.

Ling, B.C., Wu, J., Miller, S.J., Monk, K.R., Shamekh, R., Rizvi, T.A., Decourten-Myers, G., Vogel, K.S., DeClue, J.E., and Ratner, N. (2005). Role for the epidermal growth factor receptor in neurofibromatosis-related peripheral nerve tumorigenesis. Cancer Cell *7*, 65–75.

Lothe, R.A., Smith-Sorensen, B., Hektoen, M., Stenwig, A.E., Mandahl, N., Saeter, G., and Mertens, F. (2001). Biallelic inactivation of TP53 rarely contributes to the development of malignant peripheral nerve sheath tumors. Genes Chromosomes Cancer *30*, 202–206.

Mahgoub, N., Taylor, B., Le Beau, M., Gratiot, M., Carlson, K., Jacks, T., and Shannon, K.M. (1999). Myeloid malignancies induced by alkylating agents in Nf1 mice. Blood *93*, 3617–3623.

Major, I.R. (1979). Induction of myeloid leukaemia by whole-body single exposure of CBA male mice to x-rays. Br. J. Cancer *40*, 903–913.

Major, I.R., and Mole, R.H. (1978). Myeloid leukaemia in x-ray irradiated CBA mice. Nature *272*, 455–456.

Malkin, D., Jolly, K.W., Barbier, N., Look, A.T., Friend, S.H., Gebhardt, M.C., Andersen, T.I., Borresen, A.L., Li, F.P., Garber, J., et al. (1992). Germline mutations of the p53 tumor-suppressor gene in children and young adults with second malignant neoplasms. N. Engl. J. Med. *326*, 1309–1315.

Maris, J.M., Wiersma, S.R., Mahgoub, N., Thompson, P., Geyer, R.J., Hurwitz, C.G., Lange, B.J., and Shannon, K.M. (1997). Monosomy 7 myelodysplastic syndrome and other second malignant neoplasms in children with neurofibromatosis type 1. Cancer *79*, 1438–1446.

Marsche, E. (1922). Tuberkulose und Sarkom. Zentralbl. Chir. *49*, 1057–1060.

Matesich, S.M., and Shapiro, C.L. (2003). Second cancers after breast cancer treatment. Semin. Oncol. *30*, 740–748.

Menon, A.G., Anderson, K.M., Riccardi, V.M., Chung, R.Y., Whaley, J.M., Yandell, D.W., Farmer, G.E., Freiman, R.N., Lee, J.K., Li, F.P., et al. (1990). Chromosome 17p deletions and p53 gene mutations associated with the formation of malignant neurofibrosarcomas in von Recklinghausen neurofibromatosis. Proc. Natl. Acad. Sci. USA *87*, 5435–5439.

Mertens, F., Rydholm, A., Bauer, H.F., Limon, J., Nedoszytko, B., Szadowska, A., Willen, H., Heim, S., Mitelman, F., and Mandahl, N. (1995). Cytogenetic findings in malignant peripheral nerve sheath tumors. Int. J. Cancer *61*, 793–798.

Mole, R.H., Papworth, D.G., and Corp, M.J. (1983). The dose-response for x-ray induction of myeloid leukaemia in male CBA/H mice. Br. J. Cancer *47*, 285–291.

Murray, E.M., Werner, D., Greeff, E.A., and Taylor, D.A. (1999). Postradiation sarcomas: 20 cases and a literature review. Int. J. Radiat. Oncol. Biol. Phys. *45*, 951–961.

Nakanishi, H., Tomita, Y., Myoui, A., Yoshikawa, H., Sakai, K., Kato, Y., Ochi, T., and Aozasa, K. (1998). Mutation of the p53 gene in postradiation sarcoma. Lab. Invest. *78*, 727–733.

Neglia, J.P., Meadows, A.T., Robison, L.L., Kim, T.H., Newton, W.A., Ruymann, F.B., Sather, H.N., and Hammond, G.D. (1991). Second neoplasms after acute lymphoblastic leukemia in childhood. N. Engl. J. Med. *325*, 1330–1336.

Nichols, K.E., Malkin, D., Garber, J.E., Fraumeni, J.F., Jr., and Li, F.P. (2001). Germ-line p53 mutations predispose to a wide spectrum of early-onset cancers. Cancer Epidemiol. Biomarkers Prev. *10*, 83–87.

Olshen, A.B., Venkatraman, E.S., Lucito, R., and Wigler, M. (2004). Circular binary segmentation for the analysis of array-based DNA copy number data. Biostatistics *5*, 557–572.

Papageorgio, C., Seiter, K., and Feldman, E.J. (1999). Therapy-related myelodysplastic syndrome in adults with neurofibromatosis. Leuk. Lymphoma *32*, 605–608.

Pendlebury, S.C., Bilous, M., and Langlands, A.O. (1995). Sarcomas following radiation therapy for breast cancer: a report of three cases and a review of the literature. Int. J. Radiat. Oncol. Biol. Phys. *31*, 405–410.

Pinkel, D., Segraves, R., Sudar, D., Clark, S., Poole, I., Kowbel, D., Collins, C., Kuo, W.L., Chen, C., Zhai, Y., et al. (1998). High resolution analysis of DNA copy number variation using comparative genomic hybridization to microarrays. Nat. Genet. *20*, 207–211.

Plaat, B.E., Molenaar, W.M., Mastik, M.F., Hoekstra, H.J., te Meerman, G.J., and van den Berg, E. (1999). Computer-assisted cytogenetic analysis of 51 malignant peripheral-nerve-sheath tumors: sporadic vs. neurofibromatosis-type-1-associated malignant schwannomas. Int. J. Cancer *83*, 171–178.

Preston, D.L., Kusumi, S., Tomonaga, M., Izumi, S., Ron, E., Kuramoto, A., Kamada, N., Dohy, H., Matsuo, T., Matsui, T., et al. (1994). Cancer incidence in atomic bomb survivors. Part III. Leukemia, lymphoma and multiple myeloma, 1950–1987. Radiat. Res. *137*, S68–S97.

Remmelink, M., Decaestecker, C., Darro, F., Goldschmidt, D., Gebhart, M., Pasteels, J.L., Kiss, R., and Salmon, I. (1998). The in vitro influence of eight hormones and growth factors on the proliferation of eight sarcoma cell lines. J. Cancer Res. Clin. Oncol. *124*, 155–164.

Rowley, J.D., Golomb, H.M., and Vardiman, J. (1977). Nonrandom chromosomal abnormalities in acute nonlymphocytic leukemia in patients treated for Hodgkin disease and non-Hodgkin lymphoma. Blood *50*, 759.

Sekyi-Otu, A., Bell, R.S., Ohashi, C., Pollak, M., and Andrulis, I.L. (1995). Insulin-like growth factor 1 (IGF-1) receptors, IGF-1, and IGF-2 are expressed in primary human sarcomas. Cancer Res. *55*, 129–134.

Side, L.E., and Shannon, K.M. (1998). The NF1 gene as a tumor suppressor. In Neurofibromatosis Type 1, M. Upashyaya and D.N. Cooper, eds. (Oxford: Bios Scientific Publishers), pp. 133–152.

Smith, P.G., and Doll, R. (1982). Mortality among patients with ankylosing spondylitis after a single treatment course with x rays. Br. Med. J. (Clin. Res. Ed.) *284*, 449–460.

Smith, S.M., Le Beau, M.M., Huo, D., Karrison, T., Sobecks, R.M., Anastasi, J., Vardiman, J.W., Rowley, J.D., and Larson, R.A. (2003). Clinical-cytogenetic associations in 306 patients with therapy-related myelodysplasia and myeloid leukemia: the University of Chicago series. Blood *102*, 43–52.

Snijders, A.M., Nowak, N.J., Huey, B., Fridlyand, J., Law, S., Conroy, J., Tokuyasu, T., Demir, K., Chiu, R., Mao, J.H., et al. (2005). Mapping segmental and sequence variations among laboratory mice using BAC array CGH. Genome Res. *15*, 302–311.

Stiller, C.A., Chessells, J.M., and Fitchett, M. (1994). Neurofibromatosis and childhood leukemia/lymphoma: A population-based UKCCSG study. Br. J. Cancer *70*, 969–972.

Thirman, M.J., and Larson, R.A. (1996). Therapy-related myeloid leukemia. Hematol. Oncol. Clin. North Am. *10*, 293–320.

Tucker, M.A., Coleman, C.N., Cox, R.S., Varghese, A., and Rosenberg, S.A. (1988). Risk of second cancers after treatment for Hodgkin's disease. N. Engl. J. Med. *318*, 76–81.

van Leeuwen, F.E., Klokman, W.J., Hagenbeek, A., Noyon, R., van den Belt-Dusebout, A.W., van Kerkhoff, E.H., van Heerde, P., and Somers, R. (1994). Second cancer risk following Hodgkin's disease: a 20-year follow-up study. J. Clin. Oncol. *12*, 312–325.

Vogel, K.S., Klesse, L.J., Velasco-Miguel, S., Meyers, K., Rushing, E.J., and Parada, L.F. (1999). Mouse tumor model for neurofibromatosis type 1. Science *286*, 2176–2179.

Wang, J., Coltrera, M.D., and Gown, A.M. (1994). Cell proliferation in human soft tissue tumors correlates with platelet-derived growth factor B chain expression: an immunohistochemical and in situ hybridization study. Cancer Res. *54*, 560–564.

Watson, M.A., Perry, A., Tihan, T., Prayson, R.A., Guha, A., Bridge, J., Ferner, R., and Gutmann, D.H. (2004). Gene expression profiling reveals unique molecular subtypes of Neurofibromatosis Type I-associated and sporadic malignant peripheral nerve sheath tumors. Brain Pathol. *14*, 297–303.

Weiss, S.W., Langloss, J.M., and Enzinger, F.M. (1983). Value of S-100 protein in the diagnosis of soft tissue tumors with particular reference to benign and malignant Schwann cell tumors. Lab. Invest. *49*, 299–308.

Wick, M.R., Swanson, P.E., Scheithauer, B.W., and Manivel, J.C. (1987). Malignant peripheral nerve sheath tumor. An immunohistochemical study of 62 cases. Am. J. Clin. Pathol. *87*, 425–433.

Wong, F.L., Boice, J.D., Jr., Abramson, D.H., Tarone, R.E., Kleinerman, R.A., Stovall, M., Goldman, M.B., Seddon, J.M., Tarbell, N., Fraumeni, J.F., Jr., and Li, F.P. (1997). Cancer incidence after retinoblastoma. Radiation dose and sarcoma risk. JAMA *278*, 1262–1267.

Yasui, K., Arii, S., Zhao, C., Imoto, I., Ueda, M., Nagai, H., Emi, M., and Inazawa, J. (2002). TFDP1, CUL4A, and CDC16 identified as targets for amplification at 13q34 in hepatocellular carcinomas. Hepatology *35*, 1476–1484.